Dentomaxillofacial Radiology (2021) 50, 20200559

birpublications.org/dmfr

RESEARCH ARTICLE

Fractal analysis of the trabecular bone pattern in the presence/absence of metal artifact–producing objects: Comparison of cone-beam computed tomography with panoramic and periapical radiography

[1]Bardia Vadiati Saberi, [2]Negar Khosravifard, [3]Kowsar Nooshmand, [2]Zahra Dalili Kajan and [4]Mohammad Ebrahim Ghaffari

[1]Department of Periodontics, Dental Sciences Research Center, School of Dentistry, Guilan University of Medical Sciences, Rasht, Iran; [2]Department of Maxillofacial Radiology, Dental Sciences Research Center, School of Dentistry, Guilan University of Medical Sciences, Rasht, Iran; [3]Department of Maxillofacial Radiology, School of Dentistry, Guilan University of Medical Sciences, Rasht, Iran; [4]Department of Biostatistics, Dental Sciences Research Center, School of Dentistry, Guilan University of Medical Sciences, Rasht, Iran

Objectives: The effect of metallic objects on the fractal dimension (FD), bone area fraction (BAF) and gray scale values (GSVs) of cone-beam CT (CBCT) images was assessed. Also, FD, BAF and GSV were compared among CBCT, digital periapical and panoramic radiographies.
Methods: Digital periapical and panoramic radiographs were acquired from six blocks of bovine rib. Additionally, different arrangements of titanium implants and intracanal metallic posts were created in the bone blocks and CBCT scans were taken from the different implant-root arrangements. The three radiographical modalities were compared by analysis of variance. Pairwise comparisons between the modalities were performed by the Tukey test (significance level set at 0.05).
Results: Different root-implant arrangements in the CBCT images revealed no significant differences in the FD ($p = 0.920$), BAF and GSV values ($p = 0.623$). FD differed significantly among the three modalities ($p < 0.001$). Significant differences were found between CBCT and each of the periapical and panoramic techniques ($p < 0.001$), while no remarkable differences were observed in the FD of the periapical and panoramic images ($p = 0.294$). BAF and GSV showed significantly different results among the three radiographical techniques ($p < 0.001$). The difference was remarkable between CBCT and periapical ($p < 0.001$), CBCT and panoramic ($p < 0.001$) and periapical and panoramic ($p = 0.008$).
Conclusion: Presence of titanium implants and intracanal posts does not produce different results in the fractal analysis (FA) of the CBCT images. The trabecular bone pattern is best assessed by FA of the periapical radiographs followed by the panoramic and CBCT techniques, respectively.
Dentomaxillofacial Radiology (2021) **50**, 20200559. doi: 10.1259/dmfr.20200559

Cite this article as: Vadiati Saberi B, Khosravifard N, Nooshmand K, Dalili Kajan Z, Ghaffari ME. Fractal analysis of the trabecular bone pattern in the presence/absence of metal artifact–producing objects: Comparison of cone-beam computed tomography with panoramic and periapical radiography. *Dentomaxillofac Radiol* 2021; **50**: 20200559.

Keywords: Fractals; Cancellous Bone; Cone-Beam Computed Tomography; Radiography, Dental, Digital; Radiography, Panoramic

Correspondence to: Dr Negar Khosravifard, E-mail: ngrkhosravi@yahoo.com
Received 20 November 2020; revised 06 February 2021; accepted 04 March 2021

Introduction

Assessment of the trabecular pattern of the jaw bones is of great importance to the dental practitioners. Bone morphology and trabecular architecture are evaluated during dental implantation as well as healing of intrabony lesions.[1–3] Furthermore, assessment of some systemic and metabolic conditions such as osteoporosis is mainly performed through observation of the changes in the trabecular bone pattern.[4–6]

Numerous strategies exist for assessment of the micro-structure of bone, among which histological assessments are usually considered as the gold standard. More practically, trabecular architecture is evaluated through radiographical images. Corpas et al[7] reported that radiographical bone defect depth is well linked to the histological observations, while radiographical fractal analysis (FA) does not seem to match histological FA. Moreover, they found that subtle bone changes could be detected by digital intraoral radiographs rather than cone-beam CT (CBCT). On the other hand, high-resolution CBCT has proved to have comparable results with 2D histology and micro-CT with regard to bone morphometric parameters such as trabecular number, thickness, separation and bone volume fraction.[8,9]

FA is an efficient method that evaluates irregular and complex body structures mathematically. FA has been adopted by researchers in many dental and medical allied specialties for analysis of the diagnostic images.[10] Fractal dimension (FD), bone area fraction (BAF) and gray scale value (GSV) are the main parameters calculated in the FA of the radiographical images.[11] FA has been performed on periapical, panoramic and CBCT images for various purposes including assessment of osseointegration around dental implants and monitoring of bony changes in systemic diseases such as osteoporosis and sickle cell anaemia.[3–6,10] Despite the popularity of FA as a means of trabecular bone pattern evaluation, studies that have compared the results of this technique among different radiographical modalities are scarce.[11] To the best of our knowledge, no studies so far have evaluated the FA results among the different radiographical techniques and also in the different situations of the presence/absence of metallic artifacts.

Periapical radiographs benefit from excellent spatial resolution, low cost and low amount of radiation; however, they are incapable of three-dimensional displaying of the structures. Panoramic radiography is a popular imaging choice among the dental practitioners owing to its broad anatomical coverage and relatively low amount of radiation. Nevertheless, inherent distortion and magnification are the main shortcomings of this radiographical technique. CBCT, on the other hand, has gained considerable application since it provides distortion-free, three-dimensional images with high resolution. Despite its desirable features, CBCT is adversely influenced by the metallic objects positioned within the field of view (FOV). Image quality degradation which occurs in the vicinity of the metallic objects jeopardizes certain diagnostic tasks including the evaluation of osseointegration around dental implants, assessment of peri-implant bone defects, and peri-radicular lesions associated with endodontically treated teeth.[11–13] Furthermore, GSV of the CBCT images shows large errors when used quantitatively for bone density measurements compared to CT numbers. It is assumed that the relatively large amount of noise, different types of artifacts, and the cone-beam geometry are the main sources of inaccuracy of the CBCT gray values for quantitative bone density measurements.[14]

The present study was conducted to determine whether the presence/absence of different metallic objects yields variable results in the FA parameters of the CBCT images and to compare the results with those of digital periapical and panoramic radiographs of the same regions of interest (ROIs).

Methods and materials

Sample preparation

The present study was an experimental research which was conducted *in vitro* and approved by the Research Ethics Committee of Guilan University of Medical Sciences (approval ID: IR.GUMS.REC.1399.490). Six fresh bovine rib bone blocks measuring 5 mm × 2 cm × 2 cm were prepared. Initially, digital periapical radiographs were taken from the bone blocks to ensure proper trabecular quality and absence of already existing intrabony defects or lesions. 12 Titanium implants (3.8 × 10 mm, IFI DIO, Korea) and 24 maxillary central incisor teeth were used to be inserted in the bone blocks. The teeth had been extracted due to periodontal problems and had no evidence of root crack or resorption. Roots of the teeth were cut and shortened from the CEJ so that the total root length would be 10 mm. 12 stainless-steel intracanal posts (size M, Nordin, Montreux, Switzerland) were used to be passively inserted in half of the tooth roots. Proper fit of the intracanal posts with the root canals was confirmed by taking periapical radiographs.

Radiographical examinations

All six bone blocks underwent digital periapical, panoramic, and CBCT examinations. Since the presence/absence of metallic objects in the periapical and panoramic images does not yield any different results, these two radiographical techniques were taken only once from each bone block. On the contrary, CBCT images were taken from different arrangements of roots and implants such that each bone block underwent six different root/implant arrangements as follows: 1) Implant–Implant, 2) Implant–Root without post, 3) Implant–Root with post, 4) Root without post–Root

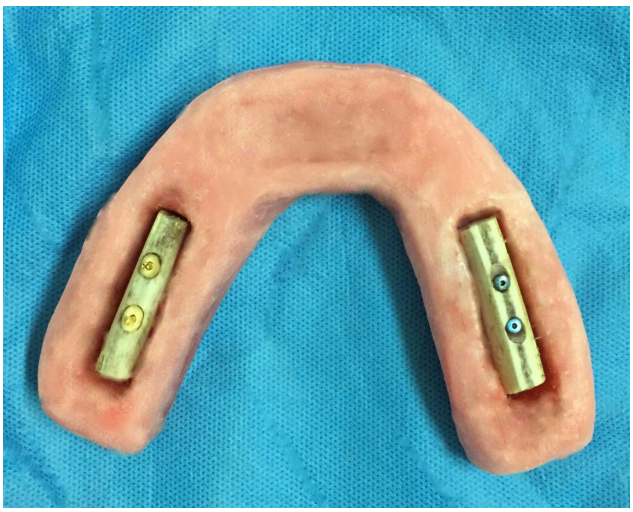

Figure 1 Two bone blocks placed in the wax arch: on the left side, two roots with posts are inserted in the bone and on the right side, two implants are placed.

without post, 5) Root without post–Root with post, and 6) Root with post–Root with post. The different arrangements of roots and implants were created to assess the influence of different metallic structures on the FA parameters of the CBCT images.

The distance between the two elements of each arrangement was precisely set at 3 mm. A wax arch was fabricated in the shape of the mandibular arch to properly simulate the dental arch shape and soft tissue density. Two spaces equal to the size of the bone blocks were created in the posterior portions of the right and left sides of the wax arch to insert the bone blocks (Figure 1).

Acquisition of the radiographical images was such that six digital periapical, six panoramic, and 36 CBCT scans were totally obtained (Figure 2). Table 1 describes the pattern of image acquisitions.

Periapical radiographs were taken with the paralleling technique by an intraoral X-ray device (Minray, Soredex, Tuusula, Finland) with exposure settings of 70 kV, 7 mA, and 0.32 s. PSP plates were used as the image receptors (Digora Optime, Soredex, Tuusula, Finland) and were processed and viewed by Scanora imaging

Table 1 Acquisition pattern of the radiographical images

	Number of the acquired imagesa		
Bone block	*Periapical*	*Panoramic*	*CBCT*
1	1	1	6
2	1	1	6
3	1	1	6
4	1	1	6
5	1	1	6
6	1	1	6
Total	6	6	36

[a]CBCT images were acquired from the six root/implant arrangements of each bone block, while periapical and panoramic radiographs were taken only once from each bone block since metallic objects do not produce any image artifacts in these two radiographical modalities

software (V.4.3.1, Digora Optime, Soredex, Tuusula, Finland).

Panoramic examinations were performed by placing the wax arch in a standard, fixed position on the chin rest of the device (Pax-i, Vatech, Hwaseong, Korea). The focal trough indicator line was adjusted on the presumed canine area of the wax arch. All exposures were taken at 73 kV, 10 mA, and 19 s. The captured images were processed and viewed by EasyDent V4 viewer (V.4.1.4.1, Vatech, Hwaseong, Korea).

CBCT images were obtained by a Pax-i 3D device (Vatech, Hwaseong, Korea) by placing the wax arch in a standard, central position on the device chin rest. During the acquisition of CBCT images, only one bone block was placed inside the wax arch in order to avoid the artifacts from the contralateral metallic inclusions. The exposure protocol for all CBCT examinations included 95 kV, 5.2 mA, 90 × 120 mm FOV, and 0.2 mm voxel size. Images were reconstructed and viewed by Ez3D-i software (Vatech, Hwaseong, Korea). Tangential sections with mesio-distal orientation were created by the "section" tool of the software in order to have similar views as the periapical and panoramic images.

Image analysis

Since we intended to investigate the area between the root and/or implant in each bone block, rectangular-shaped ROIs having 3 mm width and 10 mm length were

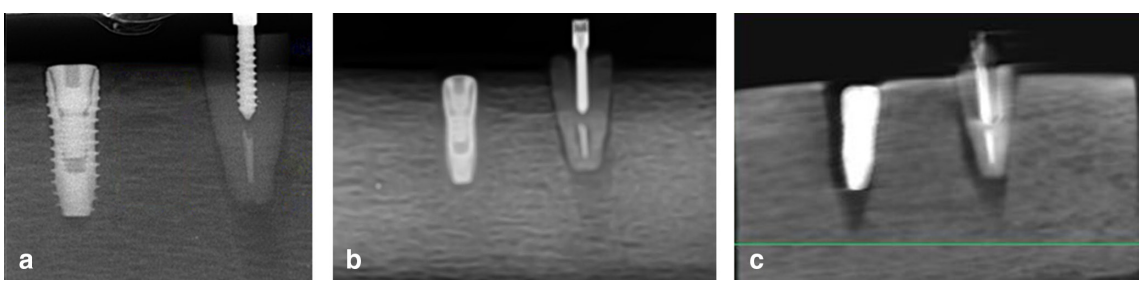

Figure 2 Different radiographical modalities of a bone block with an implant and a root having an intracanal post: (A) periapical view, (B) panoramic view, (C) CBCT.

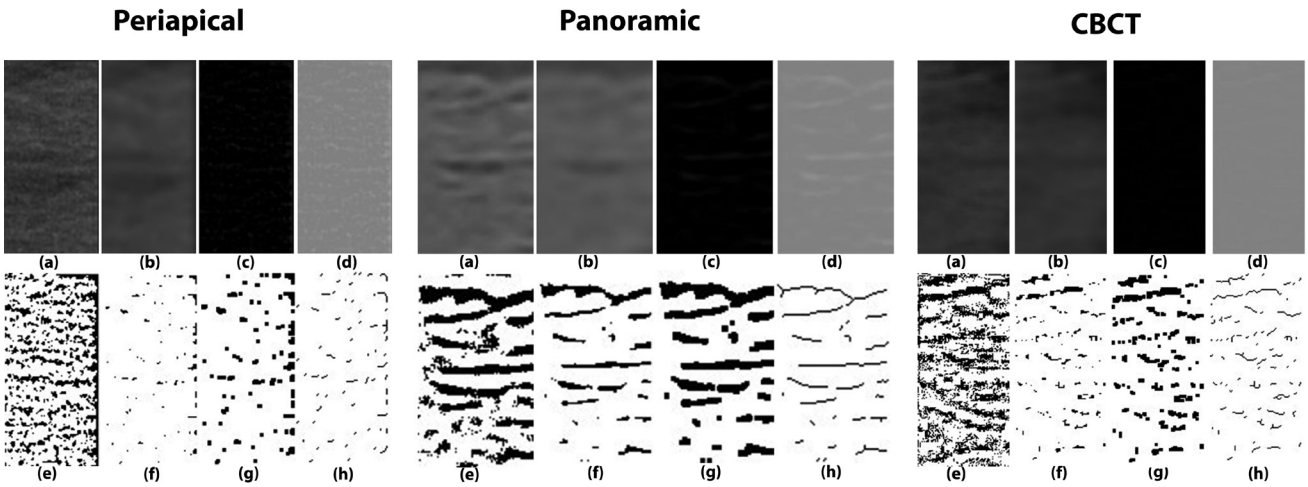

Figure 3 Steps of FD calculation on a selected ROI from the periapical, panoramic, and CBCT images: (a) ROI selection, (b) Gaussian blurring, (c) image subtraction, (d) adding 128, (e) binary image, (f) erosion, (g) dilation, (h) skeletonization.

selected. This guaranteed the incorporation of bone located between the whole length of the implant and/or root. ROIs avoided the implant and root surfaces. It is noteworthy to mention that for the periapical and panoramic radiographs, the image size was calibrated with the real object size prior to the selection of ROIs. In the CBCT images, a tangential mesio-distally oriented slice that had a thickness of 3 mm was created to cover the interspace between the implant and/or root.

Eventually, six ROIs on the periapical, six ROIs on the panoramic, and 36 ROIs on the CBCT images were prepared to be analyzed. Processing of the images was performed based on a technique introduced by White and Rudolph[15]: Images of the ROIs were transferred to the ImageJ 1.50i software (National Institutes of Health, USA). Images were Gaussian blurred with a sigma value of 3 to overcome variations in the brightness of the images. The resulting image was subtracted from the original one and a GSV of 128 was added. This resulted in the discrimination of the trabecular structures from the bone marrow spaces. Afterwards, the binary image was created. At this point, BAF and GSV were automatically calculated on the binary image by the software. Consequently, the binary image was eroded to eliminate the image noise and dilated to emphasize the outlines of the structures. The next step was the skeletonization of the ROI to prepare it for FD calculation (Figure 3). FD calculation was fulfilled with the box counting method. Boxes of 2–64 pixel dimensions were applied to the ROIs. Number of the counted plates was plotted against the total number of the plates. Eventually, FD was calculated as the slope of the regression line passing through the data points.

After two weeks, FD, BAF, and GSV values were calculated once more on new ROIs from half of the samples and the results were identical to the first measurements.

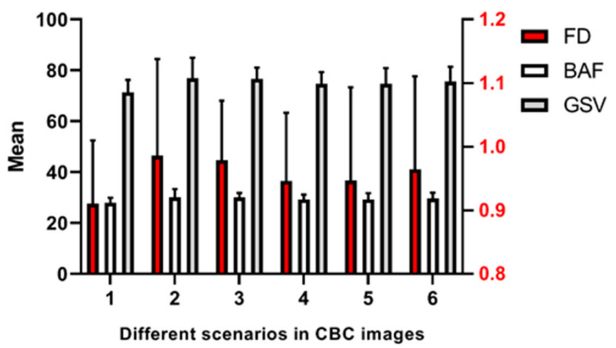

Figure 4 Mean values of the FD, BAF, and GSV on the CBCT images (1: Implant–Implant, 2: Root with post–Root with post, 3: Implant–Root without post, 4: Implant–Root with post, 5: Root without post–Root with post, 6: Root without post–Root without post)

Statistical analysis

Data were transferred to the SPSS software v.24.0 (IBM Co., Armonk, NY, USA). Initially, the hypotheses related to the parametric test methods were assessed. Accordingly, Shapiro-Wilk test confirmed normality of the data and Levon's test confirmed homogeneity of variance. Hence, data interpretation was performed by the analysis of variance (ANOVA) and pairwise comparisons between the radiographical modalities were made by the Tukey test. $p < 0.05$ was considered to indicate statistical significance.

Results

FD, BAF, and GSV values were measured for six periapical, six panoramic, and 36 CBCT images that were obtained from the bone blocks. Figure 4 and Table 2 show the mean values for the FD, BAF, and GSV of the CBCT images. Equal values of the first and second measurements suggested excellent (100%) intra observer reliability.

Table 2 Mean ± SD values of the FD, BAF, and GSV of the CBCT images in the different root-implant arrangements

Arrangement	*FD (Mean ± SD)*	*BAF (Mean ± SD)*	*GSV (Mean ± SD)*
Implant–Implant	0.91 ± 0.10	28 ± 1.89	71.39 ± 4.81
Root with post–Root with post	0.99 ± 0.15	30.16 ± 3.17	76.90 ± 8.08
Implant–Root without post	0.98 ± 0.09	30.05 ± 1.74	76.63 ± 4.44
Implant–Root with post	0.95 ± 0.11	29.30 ± 1.79	74.72 ± 4.56
Root without post–Root with post	0.95 ± 0.15	29.29 ± 2.43	74.69 ± 6.21
Root without post–Root without post	0.96 ± 0.15	29.63 ± 2.27	75.56 ± 5.79

FD fractal dimensions, BAF bone area fraction, GSV gray scale value

Comparison of the different root–implant arrangements in the CBCT images revealed no statistically significant differences in the FD, BAF, and GSV values. Accordingly, the ANOVA test showed that the FD, BAF, and GSV values of the CBCT images are not significantly altered by changing the metallic structures within the bone. Tables 3–5 represent comparisons among the different CBCT scenarios.

The mean values for the FD, BAF, and GSV of the three radiographical modalities were calculated. Accordingly, FD values were greatest in the panoramic images, while BAF and GSV had higher amounts in the periapical radiographs (Figure 5).

Comparison of the mean ± SD values of the FD, BAF, and GSV among the radiographic modalities is provided in Table 6. For each parameter, comparison of the three imaging techniques was performed by the ANOVA test and paired comparisons were made using the Tukey analysis (Figure 6). The FD values differed significantly among the three modalities ($p < 0.001$). Pairwise comparisons revealed statistically significant differences between CBCT and periapical as well as CBCT and panoramic images ($p < 0.001$), while no remarkable difference was observed between the FD values of the periapical and panoramic radiographs ($p = 0.294$). Comparison of the BAF and GSV values showed statistically significant results among the radiographic techniques ($p < 0.001$). Also, paired comparisons revealed remarkable differences in the BAF and GSV between CBCT and periapical ($p < 0.001$), CBCT and panoramic ($p < 0.001$), and periapical and panoramic images ($p = 0.008$).

Discussion

Identification of the trabecular bone pattern is an important aspect of dental implantology, surgical planning, orthodontics, and evaluation of the healing sites.[16–20] Bone quality is highly dependent on the trabecular micro-architecture. Therefore, assessment of the trabecular pattern is essential for successful osseointegration and proper bone healing.[21–24] Furthermore, conditions such as osteoporosis and diabetes mellitus are monitored through changes observed in the trabecular architecture.[6,25]

FA has been widely used in dentistry for the study of images. The technique incorporates a mathematical approach for measurement of the structural complexity. Several parameters including FD, BAF, and GSV could be measured through such an analysis. FD is a quantitative measure of the structure's complexity. Usually, more complex structures have a higher FD. BAF is related to the percentage of the pixels that represent the trabecular pattern and GSV corresponds to the mean GSV of the pixels.[10,11,26]

Kato et al[10] performed a comprehensive review on the applications of FA in the dental images. They found that this technique had been mostly applied on the panoramic and periapical radiographs, followed by CBCT. The Image J software and the box-counting method were most frequently used. Moreover, they reported that the most common objective of the FA studies was the assessment of bone mineral density (BMD), followed by

Table 3 Comparison of the FD values of the CBCT images in the different root–implant arrangements

Arrangement	*FD (Mean ± SD)*	*F*	*p*
Implant–Implant	0.91 ± 0.10	0.28	0.920
Root with post–Root with post	0.99 ± 0.15		
Implant–Root without post	0.98 ± 0.09		
Implant–Root with post	0.95 ± 0.11		
Root without post–Root with post	0.95 ± 0.15		
Root without post–Root without post	0.96 ± 0.15		

FD fractal dimensions

Table 4 Comparison of the BAF values of the CBCT images in the different root–implant arrangements

Arrangement	*BAF (Mean ± SD)*	*F*	*p*
Implant–Implant	28 ± 1.89	0.71	0.623
Root with post–Root with post	30.16 ± 3.17		
Implant–Root without post	30.05 ± 1.74		
Implant–Root with post	29.30 ± 1.79		
Root without post–Root with post	29.29 ± 2.43		
Root without post–Root without post	29.63 ± 2.27		

BAF bone area fraction

Table 5 Comparison of the GSV values of the CBCT images in the different root–implant arrangements

Arrangement	*GSV (Mean ± SD)*	*F*	*p*
Implant–Implant	71.39 ± 4.81	0.71	0.623
Root with post–Root with post	76.90 ± 8.08		
Implant–Root without post	76.63 ± 4.44		
Implant–Root with post	74.72 ± 4.56		
Root without post–Root with post	74.69 ± 6.21		
Root without post–Root without post	75.56 ± 5.79		

GSV gray scale value

evaluation of the diseases and osseointegration of the implants.

Lee et al[1] studied the alveolar bone quality using FD of the panoramic radiographs and the implant stability quotient (ISQ). They concluded that the FD values were correlated with the bone quality, while correlation of ISQ with the morphometric parameters was not found to be significant. Similarly, μ et al[17] and Suer et al[18] stated that FD analysis could be helpful in detecting changes in the peri-implant alveolar trabecular bone pattern in clinical situations. Kulczyk et al[16] compared ISQ and FD of the alveolar bone at the implant sites using intraoral radiographs. The authors reported that no correlation was found between the two techniques in the mandible; however, a significant correlation was found in the cervical bone of the maxillary implants.

FD has also been introduced as a good discriminator of low BMD in both males and females, while the mandibular cortical width (MCW) does not perform as well.[4] Identification of the thalassemia patients' jaw bone and measurement of bone regeneration have also been mentioned as the capabilities of FD analysis of the panoramic radiographs.[3,6]

Although a large number of studies have been carried out using FA technique on the radiographic images, a main shortcoming is lack of a comparison between the different radiographic techniques with regard to the FA results. Magat and Sener[11] assessed the trabecular bone pattern by comparing the FD, BAF, and GSV values between panoramic and CBCT images. They found that although CBCT has the advantage of providing 3D images and 3D bone structure analyses, trabecular pattern could be better assessed by the application of panoramic radiographs.

To the best of our knowledge, FA results of the periapical, panoramic, and CBCT images have not been compared so far. Furthermore, the influence of metal artifacts on the image quality degradation in CBCT and the resulting FD values has not been taken into consideration. Since most fractal analyses in CBCT are related to the peri-implant bone and lesions associated with endodontically treated teeth, it is important to determine the possibility of changes in the FD values by altering the presence/absence of implants and intracanal metallic posts.

Table 6 Comparison of the mean FD, BAF, and GSV values among the periapical, panoramic, and CBCT images

	Periapical (n = 6)	*Panoramic (n = 6)*	*CBCT (n = 36)*	*F*	*P*
FD	1.16 ± 0.05	1.25 ± 0.05	0.95 ± 0.12	25.29	<0.001*
BAF	42.75 ± 1.26	38.95 ± 1.74	29.40 ± 2.22	140.48	<0.001*
GSV	109.01 ± 3.20	99.33 ± 4.43	74.98 ± 5.67	140.49	<0.001*

FD: fractal dimensions, BAF: bone area fraction, GSV: gray scale value; *Differences are significant at the 0.05 level

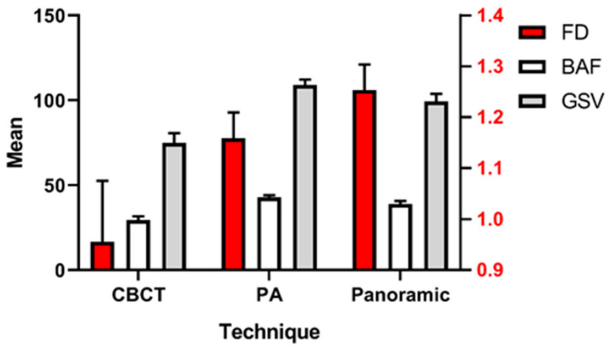

Figure 5 Comparison of FD, BAF, and GSV among the radiographic techniques

In this study, we placed titanium implants and intracanal metallic posts inside blocks of bovine rib bone. Implants and intracanal posts are the two main sources of metal artefact generation in the CBCT images of the jaw bones.[27,28] Accordingly, data corruption that takes place around the artefact sources adversely influences the image resolution. Such data loss often hardens the assessment of peri-implant bone and also bone adjacent to the teeth with intracanal metallic posts.[29] We created different conditions of the presence/absence of implants and intracanal posts as well as different arrangements to determine whether the FA results vary among the CBCT images. Furthermore, we compared the periapical, panoramic, and CBCT images in terms of the FD, BAF, and GSV measurements. Comparison of the FD, BAF, and GSV among the different CBCT scenarios revealed no significant differences ($p > 0.05$). In other words, we found that whether an implant, a root with an intracanal post, or a root without an intracanal post is present within the bone, the amounts of FD, BAF, and GSV calculated for the interspace bone do not vary significantly in the CBCT images. Therefore, presence of metallic structures does not seem to alter the FA results of CBCT.

The mean FD, BAF, and GSV values that we obtained from the CBCT images were less than those measured by Magat and Sener.[11] This difference could

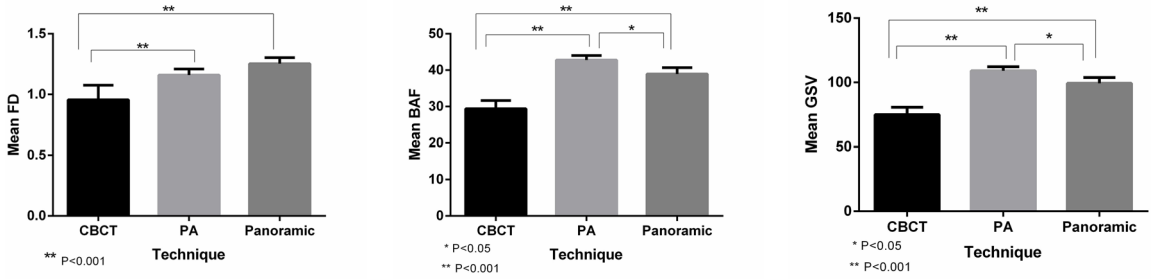

Figure 6 Pairwise comparison of the radiographic techniques in terms of FD, BAF, and GSV

be attributed to the type of bone, since we used bovine rib which has abundant bone marrow spaces while they used dry human mandibles. Also, the device type and voxel size could be further reasons for this variation.

An important feature of FA is the ROI selection. Magat and Sener,[11] mentioned human error in selecting standard ROIs as a limitation of their study. In the present study, we attempted to minimize such an error by selecting similar ROIs that were precisely located between the implants and/or roots. The ROIs measured 3 × 10 mm and avoided the implant and/or root surfaces. Considering different image resolution of the periapical, panoramic and CBCT images, ROIs of the same size would be definitely different in the number of pixels. However, we took advantage of ROIs that were related to the same bone areas. This guaranteed that the comparisons were reliably made between similar regions.

This was the first study to compare the FA results of the periapical, panoramic and CBCT images. According to the comparisons, we observed that the mean FD, BAF, and GSV varied significantly among the three modalities ($p < 0.001$). Pairwise comparisons between the techniques also revealed that CBCT had significantly lower FD, BAF, and GSV compared to each of the periapical and panoramic techniques ($p < 0.001$). BAF and GSV had significant differences between the periapical and panoramic images ($p < 0.05$) with both parameters being greater on the periapical radiographs. However, the FD values did not vary significantly between the periapical and panoramic images ($p = 0.294$). By comparing panoramic and CBCT images, Magat and Sener also concluded that the two techniques are different in terms of FD, BAF, and GSV. They suggested that the use of panoramic radiographs for assessment of the trabecular bone pattern should be continued due to superior resolution over CBCT images.[11]

There are some limitations to be mentioned for this *in vitro* study. First, we used bovine rib which although has a rich trabecular and marrow space content, does not identically represent the alveolar bone. Second, we used a slice thickness of 3 mm for the CBCT images in order to create a single image of the bone between the implant and/or root. Further studies have to be performed to investigate the effect of different slice thicknesses on the FA results. Finally, other parameters including the voxel size and exposure factors that might influence the FA results have to be investigated.

Conclusion

Within the limitations of this *in vitro* study, it is concluded that the presence/absence of titanium implants and metallic intracanal posts does not produce different FA results in the CBCT images. Also, it is concluded that the FD, BAF, and GSV values differ significantly among the periapical, panoramic, and CBCT images. Identification of the trabecular bone pattern by FA is best accomplished through the periapical radiographs followed by the panoramic and CBCT images, respectively.

REFERENCES

1. Lee D-H, Ku Y, Rhyu I-C, Hong J-U, Lee C-W, Heo M-S, et al. A clinical study of alveolar bone quality using the fractal dimension and the implant stability quotient. *J Periodontal Implant Sci* 2010; **40**: 19–24. doi: https://doi.org/10.5051/jpis.2010.40.1.19
2. Soğur E, Baksı BG, Gröndahl H-G, Sen BH. Pixel intensity and fractal dimension of periapical lesions visually indiscernible in radiographs. *J Endod* 2013; **39**: 16–19. doi: https://doi.org/10.1016/j.joen.2012.10.016
3. Jurczyszyn K, Kubasiewicz-Ross P, Nawrot-Hadzik I, Gedrange T, Dominiak M, Hadzik J. Fractal dimension analysis a supplementary mathematical method for bone defect regeneration measurement. *Ann Anat* 2018; **219**: 83–8. doi: https://doi.org/10.1016/j.aanat.2018.06.003
4. Alman AC, Johnson LR, Calverley DC, Grunwald GK, Lezotte DC, Hokanson JE. Diagnostic capabilities of fractal dimension and mandibular cortical width to identify men and women with decreased bone mineral density. *Osteoporos Int* 2012; **23**: 1631–6. doi: https://doi.org/10.1007/s00198-011-1678-y
5. Sindeaux R, Figueiredo PTdeS, de Melo NS, Guimarães ATB, Lazarte L, Pereira FB, et al. Fractal dimension and mandibular cortical width in normal and osteoporotic men and women. *Maturitas* 2014; **77**: 142–8. doi: https://doi.org/10.1016/j.maturitas.2013.10.011
6. Bayrak S, Göller Bulut D, Orhan K, Sinanoğlu EA, Kurşun Çakmak Emine Şebnem, Mısırlı M, et al. Evaluation of osseous changes in dental panoramic radiography of thalassemia

patients using mandibular indexes and fractal size analysis. *Oral Radiol* 2020; **36**: 18–24. doi: https://doi.org/10.1007/s11282-019-00372-7
7. Corpas LdosS, Jacobs R, Quirynen M, Huang Y, Naert I, Duyck J. Peri-Implant bone tissue assessment by comparing the outcome of intra-oral radiograph and cone beam computed tomography analyses to the histological standard. *Clin Oral Implants Res* 2011; **22**: 492–9. doi: https://doi.org/10.1111/j.1600-0501.2010.02029.x
8. Huang Y, Dessel JV, Depypere M, EzEldeen M, Iliescu AA, Santos ED, et al. Validating cone-beam computed tomography for peri-implant bone morphometric analysis. *Bone Res* 2014; **2**: 14010. doi: https://doi.org/10.1038/boneres.2014.10
9. Van Dessel J, Huang Y, Depypere M, Rubira-Bullen I, Maes F, Jacobs R. A comparative evaluation of cone beam CT and micro-CT on trabecular bone structures in the human mandible. *Dentomaxillofac Radiol* 2013; **42**: 20130145. doi: https://doi.org/10.1259/dmfr.20130145
10. Kato CN, Barra SG, Tavares NP, Amaral TM, Brasileiro CB, Mesquita RA, et al. Use of fractal analysis in dental images: a systematic review. *Dentomaxillofac Radiol* 2020; **49**: 20180457. doi: https://doi.org/10.1259/dmfr.20180457
11. Magat G, Ozcan Sener S. Evaluation of trabecular pattern of mandible using fractal dimension, bone area fraction, and gray scale value: comparison of cone-beam computed tomography and panoramic radiography. *Oral Radiol* 2019; **35**: 35–42. doi: https://doi.org/10.1007/s11282-018-0316-1
12. Vadiati Saberi B, Khosravifard N, Ghandari F, Hadinezhad A. Detection of peri-implant bone defects using cone-beam computed tomography and digital periapical radiography with parallel and oblique projection. *Imaging Sci Dent* 2019; **49**: 265–72. doi: https://doi.org/10.5624/isd.2019.49.4.265
13. Jacobs R, Vranckx M, Vanderstuyft T, Quirynen M, Salmon B. Cbct vs other imaging modalities to assess peri-implant bone and diagnose complications: a systematic review. *Eur J Oral Implantol* 2018; **11 Suppl 1**(Suppl 1): 77–92.
14. Pauwels R, Nackaerts O, Bellaiche N, Stamatakis H, Tsiklakis K, Walker A, et al. Variability of dental cone beam CT grey values for density estimations. *Br J Radiol* 2013; **86**: 20120135. doi: https://doi.org/10.1259/bjr.20120135
15. White SC, Rudolph DJ. Alterations of the trabecular pattern of the jaws in patients with osteoporosis. *Oral Surg Oral Med Oral Pathol Oral Radiol Endod* 1999; **88**: 628–35. doi: https://doi.org/10.1016/S1079-2104(99)70097-1
16. Kulczyk T, Czajka-Jakubowska A, Przystańska A. A comparison between the implant stability quotient and the fractal dimension of alveolar bone at the implant site. *Biomed Res Int* 2018; **2018**: 1–72018. doi: https://doi.org/10.1155/2018/4357627
17. Mu T-J, Lee D-W, Park K-H, Moon I-S. Changes in the fractal dimension of peri-implant trabecular bone after loading: a retrospective study. *J Periodontal Implant Sci* 2013; **43**: 209–14. doi: https://doi.org/10.5051/jpis.2013.43.5.209
18. Suer BT, Yaman Z, Buyuksarac B. Correlation of fractal dimension values with implant insertion torque and resonance frequency values at implant recipient sites. *Int J Oral Maxillofac Implants* 2016; ; **31**: 55–62Jan-Feb. doi: https://doi.org/10.11607/jomi.3965
19. Kwak KH, Kim SS, Kim Y-I, Kim Y-D. Quantitative evaluation of midpalatal suture maturation via fractal analysis. *Korean J Orthod* 2016; **46**: 323–30. doi: https://doi.org/10.4041/kjod.2016.46.5.323
20. Uğur Aydın Z, Toptaş O, Göller Bulut D, Akay N, Kara T, Akbulut N. Effects of root-end filling on the fractal dimension of the periapical bone after periapical surgery: retrospective study. *Clin Oral Investig* 2019; **23**: 3645–51. doi: https://doi.org/10.1007/s00784-019-02967-0
21. de Souza Santos D, Dos Santos LC. De Albuquerque Tavares Carvalho a, Leão JC, Delrieux C, Stosic T, Stosic B. multifractal spectrum and lacunarity as measures of complexity of Osseointegration. *Clin Oral Investig* 2016; **20**: 1271–8.
22. Tözüm TF, Dursun E, Uysal S. Radiographic fractal and clinical resonance frequency analyses of posterior mandibular dental implants: their possible association with mandibular cortical index with 12-month follow-up. *Implant Dent* 2016; **25**: 789–95. doi: https://doi.org/10.1097/ID.0000000000000496
23. Pârvu AE, Ţălu Ş, Crăciun C, Alb SF. Evaluation of scaling and root planing effect in generalized chronic periodontitis by fractal and multifractal analysis. *J Periodontal Res* 2014; **49**: 186–96. doi: https://doi.org/10.1111/jre.12093
24. Abdulhameed EA, Al-Rawi NH, Uthman AT, Samsudin AR. Bone texture fractal dimension analysis of Ultrasound-Treated bone around implant site: a double-blind clinical trial. *Int J Dent* 2018; **2018**: 1–10. doi: https://doi.org/10.1155/2018/2672659
25. Kurşun-Çakmak Emine Şebnem, Bayrak S. Comparison of fractal dimension analysis and panoramic-based radiomorphometric indices in the assessment of mandibular bone changes in patients with type 1 and type 2 diabetes mellitus. *Oral Surg Oral Med Oral Pathol Oral Radiol* 2018; **126**: 184–91. doi: https://doi.org/10.1016/j.oooo.2018.04.010
26. McMurphy TB, Harris CA, Griggs JA. Accuracy and precision of fractal dimension measured on model surfaces. *Dent Mater* 2014; **30**: 302–7. doi: https://doi.org/10.1016/j.dental.2013.11.015
27. Gaêta-Araujo H, Nascimento EHL, Fontenele RC, Mancini AXM, Freitas DQ, Oliveira-Santos C. Magnitude of beam-hardening artifacts produced by gutta-percha and metal posts on cone-beam computed tomography with varying tube current. *Imaging Sci Dent* 2020; **50**: 1–7. doi: https://doi.org/10.5624/isd.2020.50.1.1
28. Benic GI, Sancho-Puchades M, Jung RE, Deyhle H, Hämmerle CHF. In vitro assessment of artifacts induced by titanium dental implants in cone beam computed tomography. *Clin Oral Implants Res* 2013; **24**: 378–83. doi: https://doi.org/10.1111/clr.12048
29. Schulze RKW, Berndt D, d'Hoedt B. On cone-beam computed tomography artifacts induced by titanium implants. *Clin Oral Implants Res* 2010; **21**: 100–7. doi: https://doi.org/10.1111/j.1600-0501.2009.01817.x